

# Optical Dispersion Compensator With $>4000$ -ps/nm Tuning Range Using a Virtually Imaged Phased Array (VIPA) and Spatial Light Modulator (SLM)

Ghang-Ho Lee, *Student Member, IEEE*, Shijun Xiao, *Member, IEEE*, and Andrew M. Weiner, *Fellow, IEEE*

**Abstract**—We present an optical tunable chromatic dispersion compensator based on a virtually imaged phased-array and spatial light modulator providing both positive and negative dispersion. We demonstrate tunable dispersion compensation of 10-Gb/s positively chirped nonreturn-to-zero data signal over a range of  $-4080 \sim +850$  ps/nm (240-km single-mode fiber to 9.5-km dispersion-compensating fiber), which operates independent of the input state of polarization and has potential capability for wavelength-division multiplexing.

**Index Terms**—Dispersion compensation, optical communication, optical equalizers, wavelength-division multiplexing (WDM).

## I. INTRODUCTION

**T**UNABLE dispersion compensation is one of the most essential technologies needed for the next-generation fiber-optic communication systems. The applications will include replacing various lengths of conventional dispersion-compensating fibers (DCFs) in 10-Gb/s systems and compensating residual dispersion after the DCF to meet the tight dispersion tolerances required in 40-Gb/s and above based networks. To satisfy the future applications, the tunable dispersion compensator (TDC) must provide both positive and negative dispersion as well as large tuning range.

TDCs have been fabricated using a number of different technologies including microelectromechanical systems [1], Gires–Tournois etalons [2], fiber Bragg grating [3], wavelength-grating router [4], and virtually imaged phased array (VIPA) [5], [6]. However, the tuning range of these works is limited to  $\pm 800$  ps/nm [1]–[4], [6] or only provides negative dispersion [5]. Several of these investigations [1], [4]–[6] employed an optical signal processing approach based on parallel phase control of spatially dispersed optical frequency components [7]. The first demonstration of this approach for programmable fiber dispersion compensation was performed for subpicosecond pulses using a liquid crystal spatial light modulator (SLM) for phase control [8].

Here we employ a similar optical signal processing approach for TDC using a VIPA and SLM arranged in a reflective pulse shaper geometry [9]. We demonstrate tunable dispersion

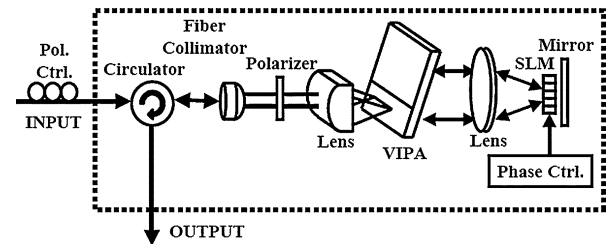


Fig. 1. Schematic of the TDC [polarizer is used for data of Fig. 2(a), (b), and Fig. 3(a), but not for Fig. 3(b)].

compensation of 10-Gb/s positively chirped nonreturn-to-zero (NRZ) data signals over a range of  $-4080 \sim +850$  ps/nm (240-km single-mode fiber (SMF) to 9.5-km DCF), which operates independent of the input state of polarization and has potential capability for wavelength-division multiplexing (WDM). Our results correspond to full tunable dispersion compensation of  $3\times$  more SMF than previously reported results [1]–[6] and should be expected to provide a tuning range of  $\pm 4080$  ps/nm without changes to the compensator setup.

## II. TUNABLE DISPERSION COMPENSATOR

The schematic of the TDC is shown in Fig. 1 [9]. It is similar to the setup in [10] but the curved mirror is replaced with an SLM to provide programmability without any moving parts. The optical input is fed into a VIPA using a lens, the VIPA spatially disperses the wavelength components within the optical input, and another lens focuses spatially dispersed wavelength components at Fourier plane. To achieve the tunable chromatic dispersion compensation, we applied a quadratic phase distribution that varies with the wavelength (spatial position) by using a standard two-layer, 128-pixel liquid crystal SLM at the Fourier plane [7]. For the experiments in Figs. 2 and 3(a), a polarizer was inserted into the TDC setup to allow programmable independent phase and amplitude control. The spatially dispersed components are recombined by the same VIPA and lens. For the experiments in Fig. 3(b), the polarizer was removed and a flipper mirror and a polarimeter were inserted between the collimator and the VIPA to tap and monitor the polarization of the incoming light. The polarization controller at the input was used to change the polarization state of incoming light and later used to prove the ability to operate the TDC independent of the input state of polarization. The periodicity of the TDC was  $\sim 49.98$  GHz, which was determined by the VIPA free spectral range (FSR), with passbands approximately centered on the ITU grid. The insertion loss for the TDC including circulator and polarization controller is around 15-dB. As a DCF module today is capable

Manuscript received February 1, 2006; revised June 13, 2006. This work was supported in part by the National Science Foundation (NSF) under Grant 0501366-ECS.

The authors are with the School of Electrical and Computer Engineering, Purdue University, West Lafayette, IN 47906-1285 USA (e-mail: leeg@purdue.edu; sxiao@purdue.edu; amw@ecn.purdue.edu).

Digital Object Identifier 10.1109/LPT.2006.880732

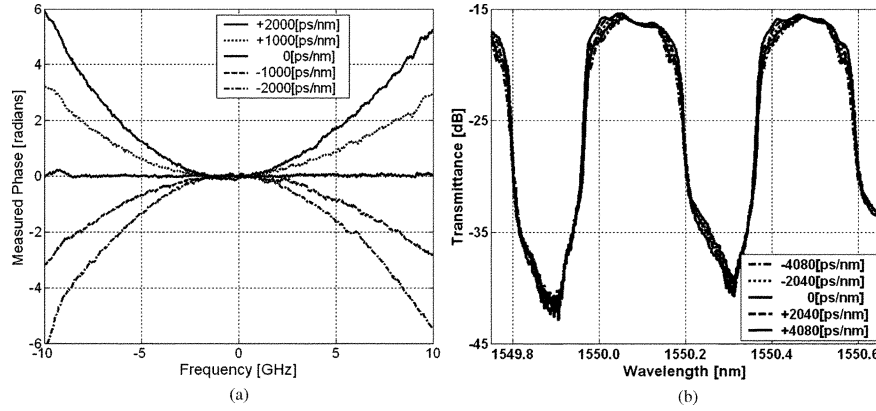


Fig. 2. (a) Measured phase with different dispersion settings (from  $-2000$  to  $+2000$  ps/nm) for TDC. (b) TDC transmission spectra with different dispersion settings (from  $-4080$  to  $+4080$  ps/nm).

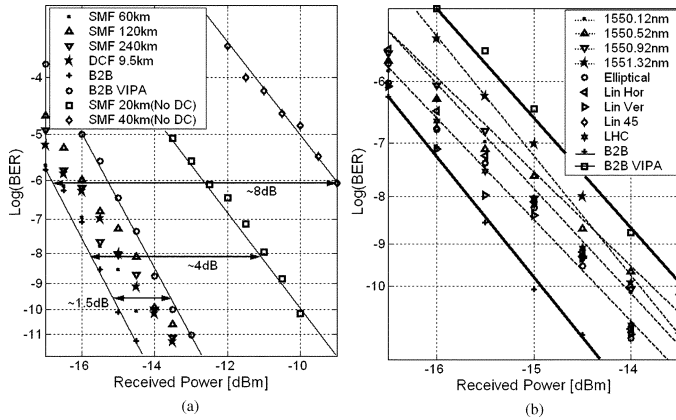


Fig. 3. TDC measurements using positively chirped 10-Gb/s NRZ ( $2^{31} - 1$ ) source. (a) BER characteristics of before and after compensation with TDC for different fiber spans. “B2B VIPA” denotes the case for 0-km transmission in Fig. 4 with TDC set to apply zero (flat) phases for entire wavelength. (b) BER characteristics for different WDM channels and different polarization after 240-km SMF transmission and TDC compensation.

of compensating 80 km of SMF transmission fiber with an insertion loss of about 6-dB, the loss of the TDC is comparable to the estimated 18-dB loss that would be incurred for compensation of a 240-km SMF span with the DCF. Other design parameters used in the TDC setup include the focal length of the semi-cylindrical lens ( $\sim 100$  mm), the input angle into the VIPA ( $\sim 2.5^\circ$ ), and the focal length of the focusing lens ( $\sim 300$  mm). The total spatial spread of the  $\sim 50$ -GHz VIPA FSR on the SLM at the Fourier plane was 7 mm which covers 70 SLM pixels.

### III. EXPERIMENTAL RESULTS

The performance of the TDC is measured in terms of the dispersion power penalty using a 10-Gb/s NRZ  $2^{31} - 1$  pseudorandom bit sequence transmission system as shown in Fig. 4. Several adjacent ITU wavelength channels around 1550 nm (1550.12, 1550.52, 1550.92, 1551.32 nm) have been applied to show potential WDM capability using the tunable transmitter. The optical source was intentionally positively chirped to have bit-error-rate (BER) characteristics as shown in Fig. 3(a), which cannot be transmitted above 40-km SMF without dispersion compensation ( $\sim 8$ -dB penalty at 40-km SMF transmission, similar characteristics as a 10-Gb/s directly modulated laser

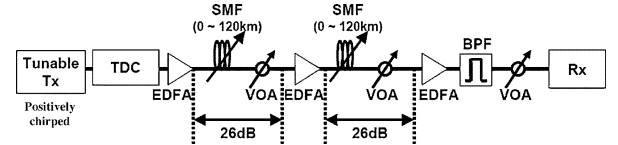


Fig. 4. Schematic of 0–240-km SMF transmission experiments testing the TDC.

system). Three erbium-doped fiber amplifiers were used to compensate the optical power loss within the system link, various lengths of fiber spools were used to generate different dispersions (20 ~ 240 km SMF with  $D = +17$  ps/nm  $\cdot$  km and 4.8 ~ 9.5 km DCF with  $D = -90$  ps/nm  $\cdot$  km) to prove the tunability of TDC in both positive and negative directions, and variable optical attenuators were placed after the fiber spools to fix the insertion loss within the fiber links to 26-dB in order to maintain constant power at the second and third optical amplifier input for different fiber lengths. For the experiments in Figs. 2 and 3(a), we have used the amplitude modulation capability of the SLM-polarizer combination, to limit the passband within the FSR to 28 GHz (41 pixels), which is large enough for 50-GHz-spaced WDM systems, and placed the wavelength channel at the middle of the passband [passband characteristics are shown in Fig. 2(b)]. This is done to ensure a linear mapping between optical frequency and spatial position (or SLM pixel number).

Within the programmed passband, the quadratic phases provided by pixel  $n$  of the SLM can be formulated as

$$\Phi(n) = \frac{\phi_{\text{quad}}}{2}(n - 21)^2(2\pi \cdot \Delta f)^2$$

and

$$(DL)_{\text{eff}} = -\frac{2\pi c \cdot \phi_{\text{quad}}}{\lambda^2} \quad (1)$$

where  $n$  is the pixel number from 1 to 41,  $\phi_{\text{quad}}$  (in squared picoseconds) is the second-order phase dispersion,  $\Delta f$  is the frequency increment between adjacent pixels (which is 0.68 GHz in our case), and  $(DL)_{\text{eff}}$  is the effective dispersion provided by our TDC setup. The phase variation is discretely sampled over the 41 pixels. The amount of chromatic dispersion applied by the TDC is determined by the quadratic phase variations within the

pixels by changing  $\phi_{\text{quad}}$  in (1). The chromatic dispersion compensation of 240-km standard SMF transmission was achieved by applying quadratic phase with maximum excursion of  $-6.3\pi$  for pixels 1 and 41 in (1). Likewise, 120- and 60-km SMF were compensated by applying the quadratic phase with maximum excursion of  $-3.3\pi$  and  $-1.8\pi$ , respectively. For the 4.8- and 9.5-km DCF, opposite signed quadratic phases with maximum excursion of  $0.4\pi$  and  $1.0\pi$  were applied. One of the significant advantages of our setup is that the SLM in TDC has close to 800 different phase levels within the  $0-2\pi$  range which can be programmed by using a laboratory PC and allow us to apply accurate values of chromatic dispersion needed in the system.

Characterization measurements of the TDC are shown in Fig. 2. Fig. 2(a) shows examples of the spectral phase response measured by modulating a microwave tone onto a CW laser, which is passed through the TDC, detected, and analyzed by a vector network analyzer over a 20-GHz optical band for several dispersion settings from  $-2000$  to  $+2000$  ps/nm. The detailed experimental setup can be found in [12]. The results confirm that clear quadratic phase functions can easily be applied. In some cases, evidence of small phase steps can be observed at large phase shifts (e.g.,  $6 \sim 10$  GHz region of  $+2000$  ps/nm). These steps correspond to the individual pixels in the SLM and can, in principle, be smoothed by reducing the spectral resolution of the VIPA based TDC. Fig. 2(b) shows the transmission spectra for the TDC with different dispersion settings ranging from  $-4080$  to  $+4080$  ps/nm with the passband intensity limited to 28 GHz as mentioned earlier. No significant changes in the transmission spectrum were observed. The insertion loss deviation was less than 2 dB over the full range of the TDC tested. This indicates the capability of programmable wavelength-dependent phase response with a relatively flat amplitude response that depends only weakly on wavelength and programmed dispersion. These are important features needed for tunable dispersion compensating modules.

The chromatic dispersion compensation system experiment results for various fiber lengths (60 km, 120 km, 240-km SMF, and 9.5-km DCF) using TDC are shown in Fig. 3(a). The results show error-free transmission, with the power penalty kept below 1-dB in all cases. The  $\sim 1.5$ -dB power penalty between the setup without the TDC (B2B) and with the TDC setup but with the SLM phase set to a constant (B2B VIPA) is partly due to additional components in the setup (three optical amplifiers), and partly due to the residual dispersion in the VIPA-based TDC. The latter can be further reduced (or eliminated) by carefully aligning the VIPA-lens separation. However, we performed experiments without fully eliminating such residual dispersion because it can be removed, if desired, by applying a small negative quadratic phase on the SLM.

We performed the 240-km transmission tests for several different polarization states (namely, arbitrary elliptical, linear horizontal, linear vertical, linear  $45^\circ$ , left-hand circular). For these experiments, the polarizer was removed and a flipper mirror and a polarimeter were inserted between the collimator and the VIPA. The liquid crystal layers were programmed in common-mode (explained in detail in [11]), which provides an isotropic polarization-independent phase control [11]. No additional adjustments were made at the TDC for the different polarization states. The results in Fig. 3(b) show that the dependence of the power penalty due to the different input polarizations is negligible (less than  $\sim 0.5$  dB). We also repeated the 240-km

transmission tests for four adjacent 50-GHz-spaced wavelength channels. Similar error-free transmission has been achieved, as shown in Fig. 3(b), which shows potential WDM capability of the TDC if the VIPA FSR is matched to the WDM channel spacing.

#### IV. CONCLUSION

We have demonstrated a TDC which can provide accurate chromatic dispersion compensation of  $-4080 \sim +850$  ps/nm which operates independent of the input state of polarization and has potential WDM capability. This is, to our best knowledge, the largest tuning range achieved for a tunable chromatic dispersion compensator with optical TDC. Furthermore, because both the transmission spectra and the BER curves remain well behaved over the full range of fiber lengths and dispersion tested, we believe that extension to compensation of even larger amount of dispersion is possible.

#### ACKNOWLEDGMENT

The authors would like to thank Dr. D. E. Leaird for technical discussion and experimental support, Avanex Corporation for providing the VIPA and SMF, Corning Incorporated and Ciena for providing the SMF.

#### REFERENCES

- [1] T. Sano, T. Iwashima, M. Katayama, T. Kanie, M. Harumoto, M. Shigehara, H. Suganuma, and M. Nishimura, "Novel multichannel tunable chromatic dispersion compensator based on MEMS and diffraction grating," *IEEE Photon. Technol. Lett.*, vol. 15, no. 8, pp. 1109–1100, Aug. 2003.
- [2] B. J. Vakoc, W. V. Sorin, and B. Y. Kim, "A tunable dispersion compensator comprised of cascaded single-cavity etalon," *IEEE Photon. Technol. Lett.*, vol. 17, no. 5, pp. 1043–1045, May 2005.
- [3] Y. W. Song, D. Starodubov, Z. Pan, Y. Xie, A. E. Willner, and J. Feinberg, "Tunable WDM dispersion compensation with fixed bandwidth and fixed passband center wavelength using a uniform FBG," *IEEE Photon. Technol. Lett.*, vol. 14, no. 8, pp. 1193–1195, Aug. 2003.
- [4] C. R. Doerr, D. M. Marom, M. A. Cappuzzo, E. Y. Chen, A. Wong-Foy, L. T. Gomez, and S. Chandrasekhar, "40-Gb/s colorless tunable dispersion compensator with 1000-ps/nm tuning range employing a planar lightwave circuit and a deformable mirror," presented at the OFC Conf., Anaheim, CA, 2005, Postdeadline paper PDP5.
- [5] L. D. Garrett, A. H. Gnauck, M. H. Eiselt, R. W. Tkach, C. Yang, C. Mao, and S. Cao, "Demonstration of virtually-imaged phased-array device for tunable dispersion compensation in  $16 \times 10$  Gb/s WDM transmission over 480 km standard fiber," in *Proc. OFC Conf.*, 2000, vol. 4, pp. 187–189.
- [6] H. Ooi, K. Nakamura, Y. Akiyama, T. Takahara, T. Terahara, Y. Kawahata, H. Isono, and G. Ishikawa, "40-Gb/s WDM transmission with Virtually Imaged Phased Array (VIPA) variable dispersion compensators," *J. Lightw. Technol.*, vol. 20, no. 12, pp. 2196–2203, Dec. 2002.
- [7] A. M. Weiner, "Femtosecond pulse shaping using spatial light modulators," *Rev. Sci. Instrum.*, vol. 71, pp. 1929–1960, 2000.
- [8] C.-C. Chang, H. P. Sardesai, and A. M. Weiner, "Dispersion-free fiber transmission for femtosecond pulses using a dispersion-compensating fiber and a programmable pulse shaper," *Opt. Lett.*, vol. 23, pp. 283–285, 1998.
- [9] G.-H. Lee and A. M. Weiner, "Programmable optical pulse burst manipulation using a virtually imaged phased array (VIPA) based Fourier transform pulse shaper," *J. Lightw. Technol.*, vol. 23, no. 11, pp. 3916–3923, Nov. 2005.
- [10] M. Shirasaki, "Compensation of chromatic dispersion and dispersion slope using a virtually imaged phased array," in *Proc. OFC Conf.*, 2001, vol. 2, pp. TuS1-1–TuS1-3.
- [11] R. D. Nelson and A. M. Weiner, "Programmable polarization-independent spectral phase compensation and pulse shaping," *Opt. Express*, vol. 11, pp. 1763–1769, 2000.
- [12] S. Xiao and A. M. Weiner, "Programmable photonic microwave filters with arbitrary ultra wideband phase response," *IEEE Trans. Microw. Theory Tech.*, submitted for publication.